

**Paper 85-3** has been designated as a Distinguished Paper at Display Week 2018. The full-length version of this paper appears in a Special Section of the *Journal of the Society for Information Display (JSID)* devoted to Display Week 2018 Distinguished Papers. This Special Section will be freely accessible until December 31, 2018 via:

[http://onlinelibrary.wiley.com/page/journal/19383657/homepage/display\\_week\\_2018.htm](http://onlinelibrary.wiley.com/page/journal/19383657/homepage/display_week_2018.htm)

Authors that wish to refer to this work are advised to cite the full-length version by referring to its DOI:

<https://doi.org/10.1002/jsid.644>

# Image-Content-Adaptive Color Breakup Index for Field-Sequential-Color Displays Using Dominant Visual Saliency Method

**Ying-Ju Lin\***, Zong Qin, Fang-Cheng Lin, Han-Ping D. Shieh, Yi-Pai Huang

Department of Photonics, College of Electrical and Computer Engineering,  
National Chiao Tung University, Hsinchu, Taiwan, 30010, R.O.C

## Abstract

Proposing an unprecedented color breakup (CBU) evaluation index based on dominant visual saliency of natural images for field-sequential-color displays, this paper achieves a linear correlation coefficient of 0.82 between subjective and objective CBU visibilities. Consequently, this study is promising for being a criterion to assess CBU in FSC-related devices—low power and virtual/augmented reality displays.

## Author Keywords

Field-sequential-color, color breakup, visual saliency

## 1. Introduction

Field-sequential-color (FSC) displays, as shown in Fig. 1(a), sequentially flash multiple fields of primary colors to produce temporal-mixing colors without using color filters. FSC displays have merits of higher light utilization efficiency and higher spatial resolution compared with spatial-color-mixing displays, e.g., conventional liquid crystal displays (LCDs) [1]. Moreover, the FSC scheme is necessary for virtual-reality (VR) and augmented-reality (AR) devices that use reflective displays, e.g., liquid crystal on silicon (LCoS) and digital mirror-devices (DMDs) [2]. However, since a relative velocity between displayed images and the observers' eyes causes that the sequentially produced primary-color images cannot perfectly overlap on the retina, FSC displays suffer from a severe issue—color breakup (CBU), which degrades image quality and discomforts observers [3]-[5], as shown in Fig. 1(b).

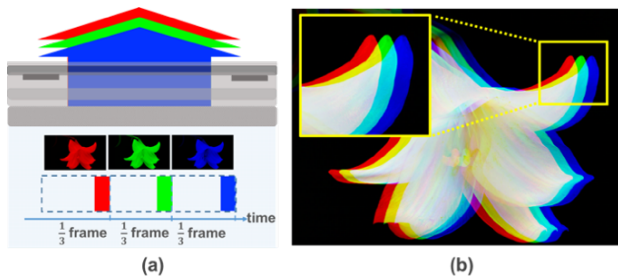


**Fig. 1.** (a) Temporal color mixing principle of FSC displays; (b) demonstration of the CBU phenomenon.

To suppress CBU, on the one hand, a number of FSC algorithms have been proposed by addressing different aspects of the causes of CBU, such as stencil-FSC [3], local primary desaturation (LPD) [4], among others. On the other hand, an objective CBU index that can accurately predict the perceptual CBU visibility according to the observers' subjectivities is highly demanded to evaluate the performances of FSC displays. Zhang *et al.* [5] and Cheng *et al.* [6] used the configuration of an FSC display, such as the color and lightness differences between the fields, to derive the CBU visibility for a simple pattern, e.g., a solid-colored block, and obtained objective results matched well with subjective results. In addition, Kim *et al.* [7] and Yang *et al.*

[8] divided an image into multiple blocks and used solid-colored blocks to approximate to the blocks, to estimate the CBU visibility. Nevertheless, using solid-colored blocks to approximate to an image and not considering how the human vision system comprehends an image [9] make it still an open problem that how to achieve an image-content-adaptive CBU index that can directly predict perceptual CBU visibilities for natural images. By considering that the CBU visibility considerably varies with image contents, such an extension from simple patterns to natural images is of great significance.

In this paper, to develop an image-content-adaptive CBU index, an image database containing 25 reference images that cover a wide range of structural and chromatic complexities is first established. For each reference image, five different levels of CBU are created and corresponding sequential fields are derived, so that 125 test cases with a variety of CBU visibilities are generated. For each test case, its fields are sequentially shown on a 240-Hz LCD, so as to obtain an FSC LCD with a frame rate of 60 Hz. Next, on the one hand, 18 subjects are asked to subjectively rate CBU visibilities of the test cases. On the other hand, with the aid of the visual saliency theory, by extracting the CBU information in the dominant visual saliency regions (DVS regions) of an image that are assumed to influence the perception of CBU the most, this work develops an objective algorithm that can calculate a CBU index from two retinal images with and without CBU respectively. By analyzing the subjective and objective results, the Pearson linear correlation coefficient (PLCC) is as high as 0.82, while not considering DVS region can only achieve a PLCC lower than 0.45, which verifies our proposal that the CBU visibility is mainly determined by the CBU information in DVS regions.

## 2. Methods

### 2.1 Establishment of CBU Image Database

To our knowledge, few acknowledged databases of natural images for CBU visibilities have been proposed. Therefore, we seek to establish one containing dozens of reference images that cover a wide range of structural and chromatic complexities, and test cases of various CBU visibilities are also desired. For this purpose, 15 complicated reference images from the ESPL Synthetic Image Database [10] are first selected. Next, ten reference images with relatively simple structures, are selected from the previous studies of CBU visibility [3-6] and Internet. Fig. 2(a) shows all the 25 reference images.

To evaluate structural complexities (SC) of the 25 reference images, multi-scale structural similarity (MS-SSIM), a method for assessing the similarity between two grayscale images [9], is adopted. First, each reference image is transferred into CIE  $L^*a^*b^*$  color space. The similarity  $SM(L^*)$  ( $0 < SM(L^*) < 1$ ) between each reference image's  $L^*$  channel and its average  $L^*$  is calculated by MS-SSIM, where a larger value indicates a

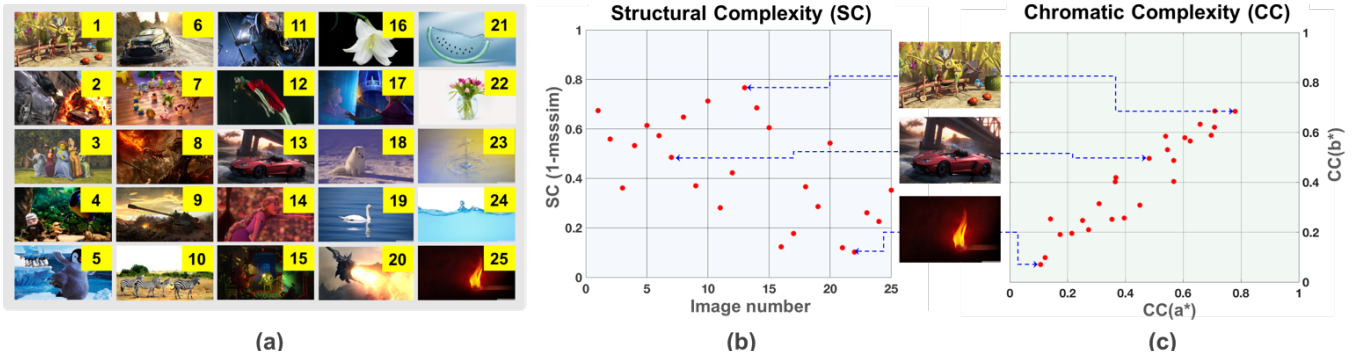


**Fig. 2.** (a) Our natural image database and assessment of the variety of differences by (b) structural complexity and (c) chromatic complexity of the image database.

better similarity. Next, SC is defined as  $1 - SM(L^*)$ , meaning that SC ( $0 < SC < 1$ ) is an index positively correlated with the structural complexity. Fig 2(b) shows the distribution of SC of the reference images, which comprehensively covers 0 to 0.8, demonstrating a wide range of SC, and three images having high, moderate, and low SCs, respectively, are also presented. Note that no images fill in the SC range of 0.8 to 1 because natural images always have intrinsic statistical features; that is, natural images hardly give rise to completely random structures with an ultra-high SC. The chromatic complexities (CC) of the reference images are evaluated with the similar method for  $a^*$  and  $b^*$  channels, as  $CC(a^*) = 1 - SM(a^*)$  and  $CC(b^*) = 1 - SM(b^*)$ . Fig. 2(c) shows the distribution of  $CC(a^*)$  and  $CC(b^*)$  for our database, where  $CC(a^*)$  and  $CC(b^*)$  are both comprehensively distributed from 0 to 0.8. Note that  $CC(a^*)$  and  $CC(b^*)$  of an image always have close values because the complexities of  $a^*$  and  $b^*$  channels of natural images are statistically consistent.

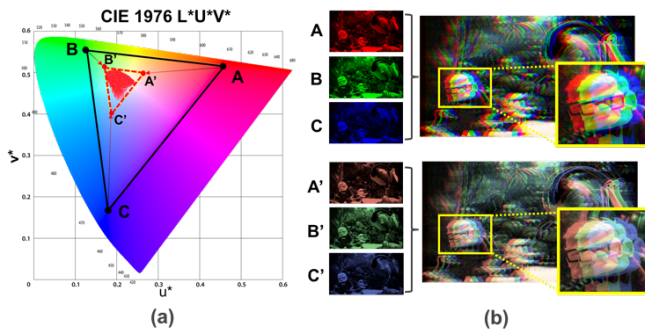


**Fig. 3.** Principle of the PD method: (a) the original (A, B and C) and new (A', B', and C') primary colors [4]; (b) the original and new fields of an image, and simulated images with different CBU performances.

After collecting the 25 reference images with a great variety of structural and chromatic complexities, this work generated several different CBU visibilities for each reference image to create diverse CBU performances. To this end, we adopt the primary desaturation (PD) method [4], which uses three new desaturated “primary” colors that can just cover the color gamut of an image to replace the original primary colors (R, G, and B). More implementation details of the PD method can be found in Fig. 3 and [4]. Obviously, the PD method can effectively suppress CBU for an image with a smaller color gamut by desaturating the fields. Therefore, we reduce saturation  $S$  of all the pixels of each reference image to 33% and 67%, respectively, and for either desaturated reference image, use the PD method to derive three

fields. Less visible CBUs are expected for the two desaturated images processed by the PD method, as the desaturation directly produces a smaller color gamut. In addition, we also use the conventional RGB scheme to derive three fields for each original and desaturated images. In this way, five test cases with different levels of CBU are generated for each reference image. For convenience, the five cases are denoted as  $PD_{S=33\%}$ ,  $PD_{S=67\%}$ ,  $RGB_{S=33\%}$ ,  $RGB_{S=67\%}$ , and  $RGB_{S=100\%}$ , respectively.

**2.2 Simulation of Retinal Images**

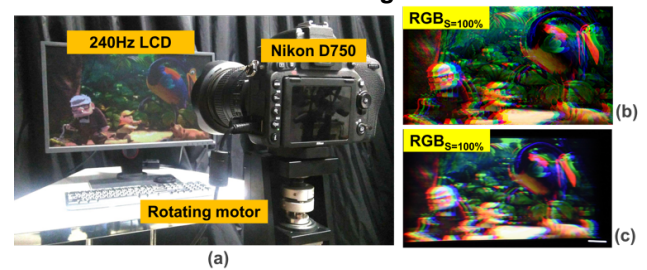


**Fig. 4.** (a) Rotating camera system. Retinal image with CBU (b) simulated by shifting the fields; (c) captured by the rotating camera system.

As mentioned before, the objective CBU assessment in this paper is based on image processing of the retinal images; hence, the retinal image with CBU needs to be simulated to know how the CBU phenomenon is perceived. Since CBU in the following experiments will be caused by horizontal saccade (very fast eye movement), the three fields of each test case are horizontally shifted and overlapped to simulate the retinal image, where the shift distance is calculated from the viewing distance and saccade speed. Fig. 4(b) shows the simulated retinal image with CBU for  $RGB_{S=100\%}$ , corresponding to a viewing distance of 1 m and saccade speed of 100 degree/s. We also actually show the three fields sequentially on a 240-Hz LCD (details will be introduced in the following part) and use a Nikon D750 camera with a 35mm-lens, assembled on a rotating motor, to capture the accumulated image in a frame time (1/60s). By placing the camera 1 m away from the display and setting the motor’s rotation speed to 100degree/s, Fig. 4(a) shows the rotating camera system, and Fig. 4(c) shows the captured image, which is almost the same as the simulated one in Fig. 4(b). By considering that the rotating camera can well imitate eye saccade, our method is accurate enough to simulate retinal images with CBU.

**2.3 Visual-Saliency-Based CBU Assessment**

After simulating the retinal images, this paper extracts the CBU

visibility from the information lying in the images. In fact, this is a generalized full-reference image quality assessment (FR-IQA) problem that evaluates the quality of a distorted image when its ideal reference image is simultaneously given. The general concept of FR-IQA is unevenly regarding the contents of an image and up-weighting the contents that highly influence an observer’s subjectivity while comparing the distorted with reference images. Recent years, the visual saliency theory makes a great success in FR-IQA [9, 11] using the information of intensity, color, orientation, among others to determine the extent that the contents in an image grab a subject’s attention. For example, the famous visual saliency-based index (VSI) has been recently proposed for general FR-IQA [9]. Inspired by this, using the effective graph-based visual saliency (GBVS) method [11], we first compute the visual saliency (VS) map of a retinal image with CBU and use this map to unevenly weight the color difference between the retinal images with and without CBU. Note that the VS map may be changed after adding CBU into the original image; i.e., the CBU “fringes” with high colorfulness may grab additional attention. Therefore, it is the image with CBU but not the one without CBU that is adopted to compute the VS map. Next, considering the effect of attention competition in color vision while watching complicated natural images [12], we propose another assumption that the overall CBU visibility is further determined by the dominant visual saliency regions (DVS regions), which are regions with VS higher than a certain threshold. In this way, the calculation flow of the proposed CBU index is plotted in Fig. 5. Note that the DVS regions contain the most severe CBU fringes, as shown by the rightmost image in Fig. 5, meaning that the proposed DVS method can effectively extract the CBU information in an image. Moreover, the color difference is in terms of Euclidean distance in the perceptually uniform CIE  $L^*a^*b^*$  color coordinate system, i.e., the vector distance between two chromas, denoted as  $\Delta C_{a^*b^*}$ . This is simply because  $\Delta C_{a^*b^*}$  is linearly associated with the perception of colorfulness, which is also the way the color difference was evaluated in the previous studies that achieved satisfactory results [5, 6].

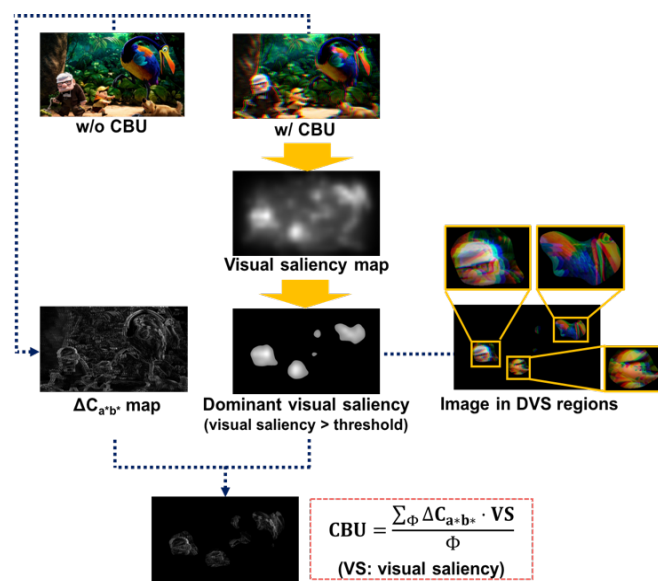


Fig. 5. Calculation flow of the proposed CBU index based on dominant visual saliency regions (DVS regions), where  $\Phi$  is the area of all the DVS regions.

### 3 Experiments and Results

#### 3.1 Conduction of Perceptual Experiments

A 24-inch LCD (BENQ XL2540) with a frame rate of 240 Hz is used in the perceptual experiments. For each test case, its three fields, followed by a black (K) field, are sequentially displayed at 240 Hz, so that an FSC LCD with a field rate of 240Hz and a frame rate is 60Hz is conducted. The viewing distance is 1 m to produce a common horizontal field of view (FOV) of 30 degrees for a 24-inch display. Two LEDs are located at left and right sides of the screen and lit alternately, to induce the subjects’ saccade within an FOV of around 30 degrees, as shown in Fig. 6(a). The saccade speed in the experiments is fixed at 100 degrees/s, leading to an alternating frequency of 1.6 Hz for the LEDs. The experiments are conducted in a dark room. 18 subjects with normal color vision (aged from 21 to 32, 8 males and 10 females) are invited to participate in the experiment. In the experiment, the 125 test cases with a variety of CBU visibilities are randomly provided, and each subject is asked to subjectively rate the CBU visibility using a 1-through-10 score table, as shown in Fig. 6(b). To ensure all the subjects can evaluate the CBU visibility correctly, a pre-training preceding the formal experiments is set for each subject, in which two vertical white bars are provided. One is rendered by sequential RGBK fields, acknowledged by the researchers to have the most severe CBU [5]; the other is rendered by successive white fields, obviously producing no CBU. In this way, each subject can understand the greatest and slightest CBU visibilities and is told to map them to score 10 and 1, respectively. Moreover, the subjects are requested to make their scores linearly correlated to their subjectivities.

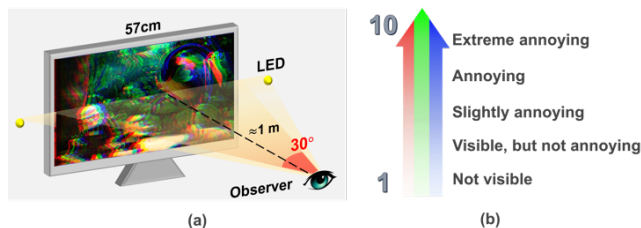
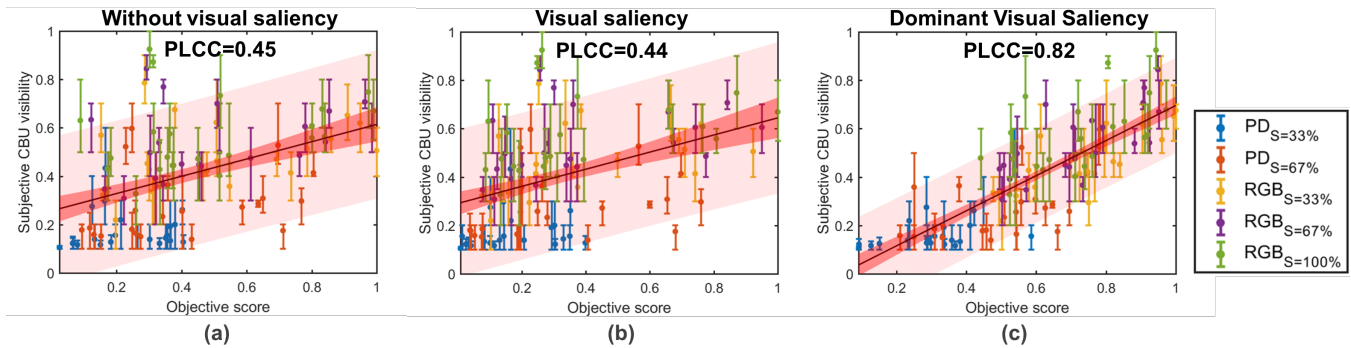


Fig. 6. (a) Architecture of the perceptual experiments. (b) Subjective score for perceptual visibility.

#### 3.2 Results

Firstly, we directly equally weight the contents in an image without using its VS map; that is, the mean  $\Delta C_{a^*b^*}$  between retinal images with and without CBU. The result is shown in Fig. 7(a), where the PLCC between the objective scores and the mean opinion scores (MOSs) is quite low, as 0.45. Subsequently, the objective CBU visibilities are calculated using the method in Fig. 5 without setting the VS threshold (VS threshold  $T=0$ ). As a result, the PLCC is still low, as 0.44, as shown in Fig. 7(b). Therefore, based on our assumption that the CBU visibility is mainly determined by DVS regions in an image, objective scores are further re-calculated by raising the VS threshold (VS threshold  $T=50\%$ ) in Fig. 5. Fig. 7(c) shows the objective results versus the subjective ones, where the PLCC is as high as 0.82, which reaches the level of mainstream FR-IQA algorithms [9], revealing that the proposed CBU index is an effective predictor for image-content-adaptive scenarios. If one uses this index to predict the subjective CBU visibility for an image with a known FSC driving scheme, Fig. 7(c) also gives the confidence and prediction intervals via linear regression on the data. In addition, by comparing the results in Figs. 7(a), (b) and (c), our assumption



**Fig.7.** Objective CBU visibilities versus subjective ones: (a) equally-weighting the contents in an image; (b) only using the original VS map; (c) using the proposed method based on dominant visual saliency (DVS). Both axes are normalized and each error bar shows mean, upper, and lower quartiles of the experimental data from the 18 subjects. The dark and light red bands denote confidence and prediction intervals with a confidence level of 90%.

that the CBU visibility is mainly determined by DVS regions is clearly verified.

#### 4 Conclusion and Discussion

To develop an image-content-adaptive CBU index, this paper first established an image database containing 25 reference images and 125 test cases covering a variety of image types and CBU levels. Based on the database, 18 subjects subjectively rated the CBU visibilities. Simultaneously, the objective results were calculated by the proposed CBU index based on DVS regions, which processed the simulated retinal images. The results showed that the objective and subjective CBU visibilities have a high PLCC of 0.82. Also, the objective CBU visibilities calculated without considering DVS regions or visual saliency have poor PLCCs of 0.45 and 0.44, respectively, demonstrating the effectiveness of DVS regions. By fitting the subjective perceptual CBU visibilities with the objective method based on dominant visual saliency, the performance of the proposed CBU index (PLCC=0.82) can be well compared with mainstream FR-IQA algorithms for general images, revealing it is an effective predictor for evaluating FSC displays, such as LCD TVs, VR and AR devices. More important, a completely image-content-adaptive CBU index which overcomes the dilemma of no application criterion for FSC displays was proposed, to our knowledge, for the first time.

In the future, we will extend our study by establishing a larger-scale image database for researchers working on FSC displays. Additionally, the computational model that how the human visual system perceives CBU will be refined to obtain a higher correlation between the subjective and objective results.

#### Acknowledgements

We thank AU Optronics Corp., Taiwan for their financial and technical supports, and iboson Technology Corp., Taiwan for conducting the rotating camera system.

#### References

- [1] H. Hasebe, and S. Kobayashi, "A Full-Color Field Sequential LCD Using Modulated Backlight," *SID Int. Symp. Dig. Tech.* **16**, 81-83 (1985).
- [2] H. W. Chen, F. W. Gou, and S.-T. Wu, "Submillisecond-Response Nematic Liquid Crystals for Augmented Reality Displays," *Opt. Mater. Express* **7(1)**, 195-201 (2017).
- [3] F. C. Lin, Y. P. Huang, C. M. Wei, and H. P. D. Shieh, "Color Breakup Reduction by 180 Hz Stencil-FSC Method in Large-Sized Color Filter-Less LCDs," *J. Disp. Technol.* **6(3)**, 107-112 (2010).
- [4] F. C. Lin, Y. N. Zhang, and E. H. A. Langendijk, "Color Breakup Suppression by Local Primary Desaturation in Field-Sequential Color LCDs," *J. Disp. Technol.* **7(2)**, 55-61 (2011).
- [5] Y. Zhang, E. H. A. Langendijk, M. Hammer, and K. Hinnen, "A New Color Breakup Measure Based on Color Difference Between Fields and Contrast to the Surrounding," *J. Disp. Technol.* **8(3)**, 145-153 (2012).
- [6] Y. K. Cheng, and H. P. D. Shieh, "Relative Contrast Sensitivity for Color Break-Up Evaluation in Field-Sequential-Color LCDs," *J. Disp. Technol.* **5(10)**, 379-384 (2009).
- [7] J. U. Kim, C. M. Yang, J. H. Bae, C. W. Kim, H. S. Lee, and D. S. Kim, "Evaluation of Static Color Breakup for Natural Images on Field Sequential Displays," *Proc. SPIE* **9015**, 90150L-1 (2014).
- [8] C. M. Yang, J. H. Bae, J. U. Kim, C. W. Kim, D. S. Kim, S. P. Cho, and H. S. Lee, "Content-Dependent Reduction of Static Color Breakup on Field Sequential Color LCDs," *J. Disp. Technol.* **12(7)**, 673-680 (2016).
- [9] Z. Qin, J. Xie, F. C. Lin, Y. P. Huang, H. P. D. Shieh, "Evaluation of a Transparent Display's Pixel Structure Regarding Subjective Quality of Diffracted See-Through Images," *IEEE Photonics J.* **9(4)**, 1-14 (2017).
- [10] D. Kundu, and B. L. Evans. "Full-Reference Visual Quality Assessment for Synthetic Images: A Subjective Study," in *2015 IEEE Conference on Image Processing*, 2374-2378 (2015).
- [11] J. Harel, C. Koch, and P. Perona, "Graph-Based Visual Saliency," in *Proceedings of the 20th Annual Neural Information Processing Systems*, 545-552 (2006).
- [12] S. Kastner, and L. G. Ungerleider. "The Neural Basis of Biased Competition in Human Visual Cortex," *Neuropsychologia* **39(12)**, 1263-1276 (2001).